https://doi.org/10.5194/egusphere-2025-6041
Preprint. Discussion started: 30 January 2026

Post-Glacial intensification of marine faulting: resolution-dependent hazard assessment

May Laor[1,2], Omri Gadol[3,4], Yizhaq Makovsky[3], Oded Katz[1], Zohar Gvirtzman[1,2]

[1]Geological Survey of Israel, Yesha'yahu Leibowitz 32, Jerusalem, Israel

[2]Institute of Earth Sciences, The Hebrew University of Jerusalem, Jerusalem, Israel

[3]The Hatter Department of Marine Technologies, Leon H. Charney School of Marine Sciences (CSMS), Haifa University, Mt. Carmel, Haifa 31905, Israel

[4]CERENA, Instituto Superior Técnico, Lisbon University, Av. Rovisco Pais, 1049-001 Lisbon, Portugal

Correspondence to: May Laor (may.laor@mail.huji.ac.il), Zohar Gvirtzman (zohar@gsi.gov.il)

Abstract

This study demonstrates how increasing stratigraphic resolution in fault hazard analysis fundamentally affects the calculated slip rates for seismic design. We investigate thin-skinned normal faults offshore Israel, that pose significant hazards to major pipelines delivering gas to onshore power plants. Previous studies, which measured displacements of a 350 ky horizon, obtained slip rates of 0.25 mm/yr. However, based on higher-resolution seismic data, here we measure displacements of a 14 ky horizon and obtain slip rates exceeding 2.4 mm/yr. This tenfold increase in recent times indicates non-linear slip rates and raises the hypothesis that the rapid post-glacial sea-level rise is the cause for the increased faulting. To examine this hypothesis, we extend

https://doi.org/10.5194/egusphere-2025-6041
Preprint. Discussion started: 30 January 2026

our time window to the latest Pleistocene, demonstrating a correlation between sea-level fluctuations and faulting variations. The subdivision of the latest Pleistocene section into glacial and interglacial cycles is based on seismic analysis integrated with principles of sequence stratigraphy. The conclusion that fault slip rates have increased after the last glacial period has double importance. First, it raises the hypothesis that rapid sea-level rise is the cause for the increased faulting - possibly due to changes in pore pressure along thin-skinned faults and detachment surfaces; this is crucial for understanding the mechanics of thin-skinned faults. Second, it highlights the importance of post-glacial stratigraphic horizons as seismic markers for fault hazard analysis, especially in circum-Mediterranean margins, where the unstable Messinian salt giant propels salt tectonics; this is crucial for geomarine hazard assessment.

1. Introduction

Building codes generally prohibit construction over active faults, but when pipelines or cables must cross active faults, two measures are recommended. First, an optimal route crossing the least hazardous faults should be selected. A method for that was recently presented by Laor and Gvirtzman (2023), who classified all faults in their study area into relative hazard levels allowing identification of the least hazardous faults. Second, site-specific surveys are needed to characterize faults that are crossed by the selected route. One way to characterize faults is to apply a probabilistic fault displacement hazard analysis (PFDHA, Youngs et al., 2003), following a probabilistic approach developed for ground motion prediction (PSHA; Cornell, 1968; McGuire, 1976; Bender and Perkins, 1987). This procedure calculates displacement hazard curves (probability versus displacement) for a given fault, based on knowledge of its earthquake recurrence intervals (magnitude-frequency relations) and the distribution of displacements. However, this knowledge is often limited and relies on weakly supported assumptions. In

https://doi.org/10.5194/egusphere-2025-6041
Preprint. Discussion started: 30 January 2026

particular, for the shallow, thin-skinned faults studied here (offshore Israel), this approach is unfeasible because it is uncertain whether these faults creep continuously or exhibit stick-slip behavior. Moreover, even in cases of stick-slip motion, magnitude-frequency relationships are unavailable, and therefore probabilistic models cannot be developed here.

In practice, site-specific surveys aiming to determine recent slip rates for seismic design measure the displacement of the youngest possible stratigraphic horizon, which is frequently 10^4 or 10^5 years old, depending on the available resolution of seismic and core/well data. Thus, hazard surveys commonly provide average slip rates representing the recent tens or hundreds of thousands of years. In this work, we demonstrate how increasing stratigraphic resolution affects fault hazard assessment. In particular, we show that slip rates after the last glacial period have increased by an order of magnitude. This somehow surprising result opens the gate for two interrelated discussions: 1) the possibility that climate-driven water and sediment loading may increase fault activity. 2) The necessity of post-glacial stratigraphic markers in marine site-specific surveys aimed for determining fault slip rates.

Our case study is the Levant continental margin, offshore Israel, which provides an ideal natural laboratory for investigating thin-skinned normal faults propelled by salt tectonics (Fig. 1). The widespread thin-skinned deformation across the Mediterranean Sea, due to the unstable Messinian salt giant, calls for reexamination of our hypothesis at additional Mediterranean sites.

https://doi.org/10.5194/egusphere-2025-6041
Preprint. Discussion started: 30 January 2026

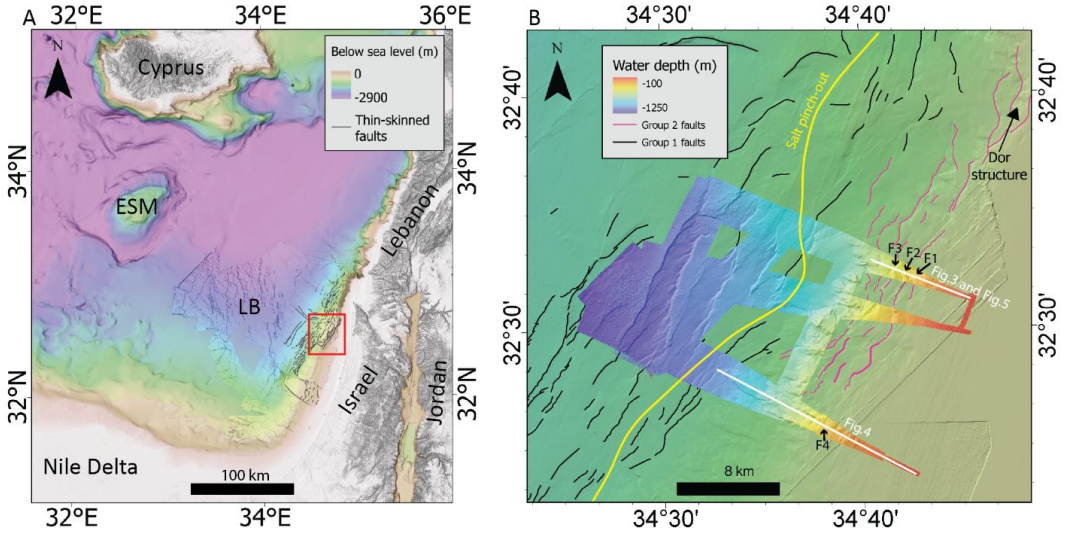

Figure 1: (A) Regional elevation map. ESM- Eratosthenes Sea Mount. LB- Levant Basin. The study area (shown in B) is marked in a red polygon. Digital elevation model from Hall (1994) and Gvirtzman et al. (2015). (B) Location map of the study area offshore northern Israel. High-resolution (20x20 m) colored bathymetric map derived from data collected for this study along the seismic survey track. Black and pink lines show faults from Groups 1 and 2, respectively (Group 2 is the focus of this study), after Laor and Gvirtzman. (2023). The yellow line indicates the salt pinch-out. White lines mark the seismic sections featured in this paper. F1-F4 denote the faults analyzed herein.

https://doi.org/10.5194/egusphere-2025-6041
Preprint. Discussion started: 30 January 2026

2. Background

2.1 Thin-skinned tectonics offshore Israel

The Israeli continental shelf and slope comprise Plio-Quaternary siliciclastic sediments derived from the Nile Delta through longshore currents (Emery et al., 1960; Gvirtzman and Buchbinder, 1978; Goldsmith and Golik, 1980; Carmel et al., 1985; Tibor et al., 1992; Buchbinder et al., 1993; Buchbinder and Zilberman, 1997; Ben-Gai et al., 2005; Frey-Martínez et al., 2006; Segev et al., 2006; Zviely et al., 2006, 2007; Klein et al., 2007; Schattner et al., 2015; Schattner and Lazar, 2016; Gadol et al., 2020; Zucker et al., 2021). This sedimentary package overlies the Messinian evaporite sequence, which lies approximately 1 km below the seafloor. The Messinian salt layer, deposited during the Messinian Salinity Crisis, reaches a maximum thickness of approximately 1.8 km in the deep basin and thins dramatically beneath the continental slope to a few tens of meters (Netzeband et al., 2006; Cartwright and Jackson, 2008; Steinberg et al., 2011; Gvirtzman et al., 2017; Manzi et al., 2018; Meilijson et al., 2018). The line at which the evaporitic sequence thins below seismic resolution is termed the salt pinch-out line (Fig. 1b; Hsü et al., 1977; Rowan et al., 1999; Ryan, 2009). Approximately 2.7 million years after cessation of salt deposition (Pliocene-Gelasian transition), continental uplift and margin tilting initiated westward salt flow, which in turn carries the overlying rock column basinward (Cartwright and Jackson, 2008; Elfassi et al., 2019; Hamdani et al., 2021). This westward motion of rocks overriding the salt relative to the stable salt-less upper slope produces extension and normal faulting.

The extensional zone exhibits hundreds of normal faults that offset the seafloor, creating tens of meters high seabed steps (Neev et al., 1976; Ben-Avraham, 1978; Garfunkel et al., 1979; Mart and Ben-Gai, 1982; Garfunkel, 1984; Garfunkel and Almagor, 1984; Tibor et al., 1992; Gradmann et

https://doi.org/10.5194/egusphere-2025-6041
Preprint. Discussion started: 30 January 2026

al., 2005; Martinez et al., 2005; Bertoni and Cartwright, 2006; Loncke et al., 2006; Netzeband et al., 2006; Mart and Ryan, 2007; Cartwright and Jackson, 2008; Clark and Cartwright, 2009; Cartwright et al., 2012; Gvirtzman et al., 2013, 2015; Katz et al., 2015; Hübscher and Netzeband, 2017; Gadol et al., 2020; Ben Zeev and Gvirtzman, 2020; Hamdani et al., 2021; Laor and Gvirtzman, 2023; Gadol et al., 2025; Laor and Gvirtzman, 2025). These faults form primarily above the salt wedge, as documented in numerous studies. However, in the Dor structure area, offshore northern Israel (Fig. 1b), a special group of listric faults is located landward of the salt pinch-out line (Fault Group 2 in Laor and Gvirtzman, 2023). These faults have been classified within the high hazard category because they are relatively big with relatively large displacements of a 350 ky horizon, indicating high slip rates relative to surrounding faults (Laor and Gvirtzman, 2023). For comparison, recent (350 kyr) slip rates of faults located above the salt wedge (Group 1 in Laor and Gvirtzman, 2023) are approximately 0.05 mm/yr (Elfassi et al., 2019; Laor and Gvirtzman, 2023), while recent (350 ky) slip rates of the big listric faults near Dor structure (Group 2; Fig. 1b) are approximately 0.25 mm/yr (Laor and Gvirtzman, 2023). Moreover, while slip rates of the salt-wedge faults have decreased from 0.11 mm/y in the Gelasian (2.6-1.8 Ma) to 0.05 mm/yr recently (350 kyr; Elfassi et al., 2019), the faults near the Dor structure reached high slip rates in the past 350 ky.

2.2. The effect of glacial and interglacial periods on thin-skinned deformation

Over the past decades, submarine mass failures have been widely investigated along continental margins and are now recognized as one of the most significant geological processes shaping continental slopes (Masson et al., 2006; Owen et al., 2007; Lee, 2009; Tappin, 2010; Katz et al.,

https://doi.org/10.5194/egusphere-2025-6041
Preprint. Discussion started: 30 January 2026

2015; Gadol et al., 2020). The mechanisms of slope failure are generally explained by a combination of preconditioning factors, such as rapid sediment accumulation, the presence of methane hydrates, the build-up of high pore-water pressures, and triggers, including seismic activity or changes in hydrostatic loading. In this context, fluctuations in sea level are increasingly considered an important factor: sea-level fall reduces hydrostatic pressure and may destabilize gas hydrates, while rapid sea-level rise enhances pore pressure and reduces slope stability (Paull et al., 1996; Maslin et al., 2004; Trincardi et al., 2003; Wien et al., 2006). Nevertheless, the global correlation between the frequency of submarine landslides and sea-level change remains debated and has not yet been unequivocally demonstrated (Urlaub et al., 2013).

Recent studies suggest that sea-level rise may affect not only sediment stability but also shallow tectonic activity. The additional water load imposed on continental shelves induces lithospheric flexure, steepening of slopes, and enhanced shear stress along fault systems (Mitrovica & Peltier, 1991). Modeling results indicate that rapid Holocene sea-level rise was sufficient to increase Coulomb failure stress by more than 1 MPa, a magnitude large enough to reactivate existing faults (Luttrell and Sandwell, 2010; Brothers et al., 2013). Observations of reservoir-induced seismicity, where rapid water loading has triggered earthquakes of up to Ms 6.5, further support the hypothesis that eustatic sea-level rise can reactivate faults along continental margins (Simpson, 1976; Talwani, 1997).

A prominent case study for the destabilization of a continental margin is the Holocene Storegga Slide offshore Norway, one of the largest documented submarine landslides. This event occurred during a period of accelerated sea-level rise, amplified by meltwater discharges from proglacial lakes Agassiz–Ojibway in North America. The combination of rapid relative sea-level rise,

https://doi.org/10.5194/egusphere-2025-6041
Preprint. Discussion started: 30 January 2026

increased pore pressure in slope sediments, and synchronous seismic activity is thought to have triggered the catastrophic failure (Bryn et al., 2005; Haflidason et al., 2005; Bondevik et al., 2012). The Storegga case thus illustrates how sea-level forcing, coupled with fault reactivation and slope instability, can jointly produce large-scale submarine failures with far-reaching geohazard implications (Smith et al., 2013).

Empirical data on the influence of sea-level fluctuations on thin-skinned marine faults remains sparse, and it is still unclear whether the same processes that destabilize continental slopes operate at larger scales in faults a few kilometers deep. Hydrostatic pressure perturbations generated by water loading and unloading cycles are known to decay rapidly at depths shallower than 1 km (Locat and Lee, 2002), while seismic monitoring typically targets deeper crustal levels. Although some elastic flexural models suggest that water loading and unloading can modulate fault slip at continental shelves, direct observational evidence is lacking. Consequently, the quantitative impact of sea-level change on shallow fault systems remains uncertain. Addressing this knowledge gap will require high-resolution geophysical data capable of distinguishing the relative roles of sea-level variability and salt tectonic processes.

2.3 Marine construction standards

Modern offshore construction standards reflect the challenges and complexities associated with installing infrastructure on the seabed, particularly in geologically dynamic settings. Unlike onshore practice, where hazard mapping and fault characterization rely on decades of established protocols, the marine environment lacks universally accepted procedures for hazard assessment and infrastructure design (Laor and Gvirtzman, 2023). This gap is largely due to the intrinsic difficulties in accessing, imaging, and dating marine faults, as well as the higher sedimentation

https://doi.org/10.5194/egusphere-2025-6041
Preprint. Discussion started: 30 January 2026

and erosion rates characteristic of many continental margins (Kvalstad, 2007; Hough et al., 2011). Consequently, decisions regarding the routing and protection of seafloor infrastructure (such as pipelines or cables) often require the integration of multiple, high-resolution seismic and bathymetric datasets, combined with site-specific geological and geotechnical investigations (Prior and Hooper, 1999; Angell et al., 2003).

A key difference in offshore geohazard assessment is the reliance on extensive seismic mapping, which is typically higher in both quality and quantity than comparable surveys on land. This abundance enables regional-to-local-scale classification of fault activity and displacement hazards without the need for exhaustive coring and stratigraphic dating for every fault encountered (Prior and Hooper, 1999; Angell et al., 2003). In practice, the inability to definitively date fault activity in the marine environment has led some standards to treat all seabed-rupturing faults as potentially active, adopting a precautionary, engineering-first approach (On, 2016). Alternatively, probabilistic analyses comparable to those used in earthquake hazard assessment have been adapted to estimate the expected frequency and size of fault displacement events, guiding both the early planning and the detailed engineering phases of offshore projects (Wong and Stepp, 1998; Youngs et al., 2003; Angell et al., 2003).

Recent approaches emphasize pragmatism and risk minimization at early planning stages. Laor and Gvirtzman (2023) propose classifying offshore faults by measurable parameters such as recent (e.g., 350 ky) vertical displacement and fault plane size, using broad seismic data coverage. This method enables infrastructure planners, working under uncertainty, to route pipelines or cables across zones of lowest apparent hazard, focusing costly site-specific studies only where unavoidable crossings occur. Such pragmatic classification provides a functional hazard map

https://doi.org/10.5194/egusphere-2025-6041
Preprint. Discussion started: 30 January 2026

explicitly designed for marine conditions, while acknowledging the current limits of fault activity characterization at sea.

Understanding recent fault displacement rates is therefore essential for developing region-specific offshore construction standards and for more accurately assessing the seismic and surface rupture hazards posed by marine faults. Improved knowledge in this area will ultimately inform the design of infrastructure and guide appropriate engineering adaptations to ensure both safety and resilience in offshore developments.

3. Methods

3.1 High-resolution seismic reflection acquisition and processing

A high-resolution multi-channel seismic survey was conducted offshore northern central Israel in June 2021 (Fig. 1). The survey consisted of eight seismic lines designed to cover the shelf edge and upper slope area (200-1200 m water depths). The seismic data were acquired using a 0.5 to 3 kHz Geo Marine Survey Systems Sparker source (Geo-Source 400) deployed with a 48-channel Geo Marine Survey Systems streamer, with a group interval of 3.25 meters. To ensure optimal spatial sampling while profiling to a depth of up to ~200 m, a multi-pinging approach was applied, including continuous recording, frequent source triggering, and post-survey trace truncation.

Raw seismic data were loaded into Emerson-Paradigm (now AspenTech SSE) software for processing and interpretation. Geometry and common midpoint (CMP) binning at a 1.56 m spacing were computed using custom MATLAB scripts and assigned to the data. Next, seismic traces were filtered to enhance signal quality, followed by amplitude scaling to balance signal strength across the dataset while preserving relative reflection amplitudes. Deconvolution steps, including de-

https://doi.org/10.5194/egusphere-2025-6041
Preprint. Discussion started: 30 January 2026

signature and de-ghosting corrections, were performed using the ECHOS DeconQ module to reduce source and receiver ghost effects. Finally, a pre-stack time migration was applied to focus reflection events and improve structural interpretation.

3.2 Horizon dating using seismo- and sequence stratigraphy

Sequence stratigraphy deals with repetitive units where the depositional conditions that prevailed during their sedimentation were similar, and they are bounded by erosional or non-depositional unconformity surfaces (Galloway, 1989). These surfaces, which separate the units, formed during sea-level fall or rise (Vail et al., 1977).

In this work, we identified unconformities that separate units with different seismic facies using seismic interpretation and horizon picking. We defined sequence boundaries (SB) according to Hunt and Tucker (1992) approach, so that they represent formation at the end of the regression. The geometry of the SB reflections truncated the top set of the former reflections by Toplap or Truncation geometry. The Truncation geometry is characterized by a high angle between the truncated reflection and the erosional reflection, and usually forms erosional topography. The Toplap geometry is characterized by a moderate angle and topography. Other criteria for SB identification are the Onlap relationship in the foreset and topset regions on the erosional surface.

3.3 Calculating the history of displacement rates

To calculate the displacement accommodated by the fault during each period, we reconstructed the displacement of the oldest horizon over time. The vertical displacement across faults was measured for each geological horizon. The relative movement of the hanging wall against the

https://doi.org/10.5194/egusphere-2025-6041
Preprint. Discussion started: 30 January 2026

223 footwall was reconstructed by calculating the cumulative offset of the earliest horizon and
224 representing it as a function of time (Fig. 2).

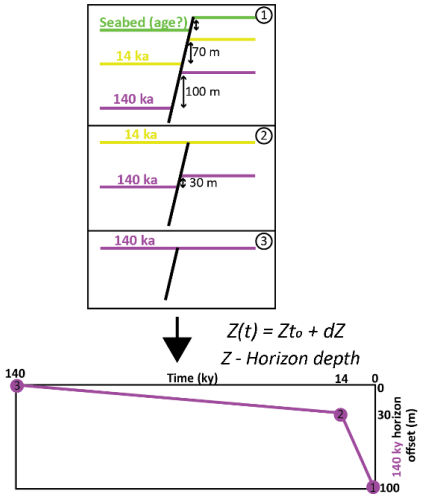

225

226 *Figure 2: The methodology for backward reconstruction of the oldest horizon movement along the*
227 *faults. The vertical offset was measured for each horizon, and the relative movement of the*
228 *hanging-wall block relative to the footwall block was reconstructed over time.*

229 Slip rates for discrete time periods were determined by dividing the incremental displacement of
230 the basal reflection by the duration of each chronostratigraphic interval. This analytical procedure
231 was applied to four faults that exhibit clear displacement of all traced horizons.

232 ## 4. Results

233 ### 4.1 Chrono-Seismo-Sequence stratigraphy

234 Figure 3 shows the division of the Plio-Quaternary section into four units based on the seismo-
235 and bio-stratigraphy of Elfassi et al. (2019), with the base of Unit 4 dated to 350 ky (light blue).

https://doi.org/10.5194/egusphere-2025-6041
Preprint. Discussion started: 30 January 2026

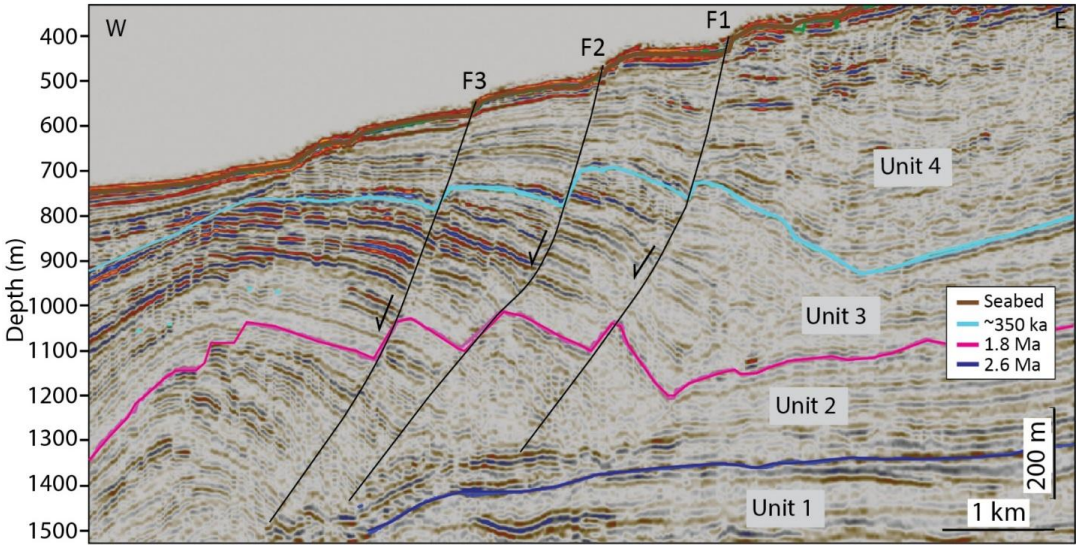

Figure 3: Seismic section from industry seismic data crossing the Group 2 faults (marked as black lines; Laor and Gvirtzman, 2023). Division of the Plio-Quaternary section into four dated units is based on Elfassi et al. (2019). Base unit 2 (blue horizon) is dated to 2.6 Ma; Base unit 3 (pink horizon) is dated to 1.8 Ma; Base unit 4 (light blue horizon) is dated to 350 ka. For the location of the line, see Figure 1.

Figure 4a further subdivides Unit 4 into four subunits (4a-4d), based on the new high-resolution survey conducted in this study (details in the Methods section above). The base of the youngest subunit 4d (yellow reflection) is interpreted as 'Surface A' identified by Neev et al. (1966), Almagor et al. (2000), Schattner et al. (2010), and Gadol et al. (2025), marking the end of the Last Glacial Maximum and the onset of sea-level rise. Recently, this horizon was further dated to approximately 14 ky (Hamman et al., 2008; Gadol et al., 2025).

https://doi.org/10.5194/egusphere-2025-6041
Preprint. Discussion started: 30 January 2026

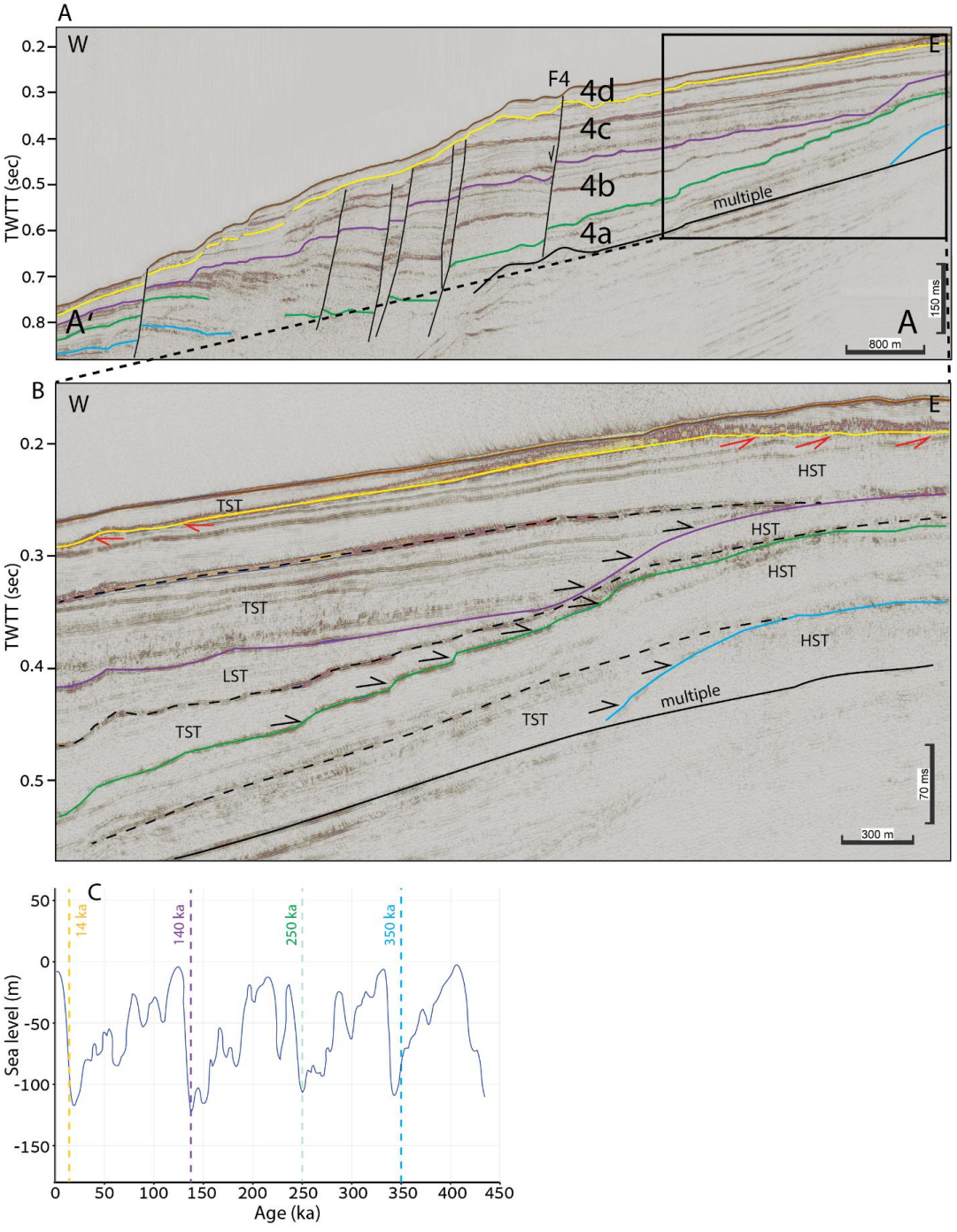

249

https://doi.org/10.5194/egusphere-2025-6041
Preprint. Discussion started: 30 January 2026

Figure 4: (A) Subdivision of Unit 4 into four sub-units (4a-4d), based on a new high-resolution seismic survey conducted in this study. Light blue horizon is dated to 350 ka (following Elfassi et al., 2019); green horizon is dated to 250 ka (based on C); purple horizon is dated to 140 ka (based on C); and the yellow horizon is dated to 14 ka (Neev et al., 1966; Almagor et al., 2000; and Schattner et al., 2010; Gadol et al., 2025) (B) Detailed view of the shelf edge zone showing geometries that were used to divide the section into sequences according to sequence stratigraphic theory. (C) Global sea level curve showing glacial and interglacial cycles. Note the four sea-level drops at approximately 350 ka, 250 ka, 140 ka, and 20 ka, which are used as sequence boundaries.

Based on sequence-stratigraphic principles, we identified the four horizons picked within Unit 4 as SBs underlain by truncations (red arrows; Fig 4b) of high-stand systems tracts (HST) and overlain by onlap geometry (black arrows; Fig 4b) of transgressive systems tracts (TST). Since all four horizons represent low sea level, and the yellow and turquoise horizons are dated to 14 ka and 350 ka, respectively, we interpret the intermediate horizons to 250 ka (green) and 140 ka (purple), respectively, according to the global sea-level curve (Fig. 4c). In summary, we now have four dated horizons corresponding to four major sea-level drops within the last 350 ky (Figure 4a-5).

https://doi.org/10.5194/egusphere-2025-6041
Preprint. Discussion started: 30 January 2026

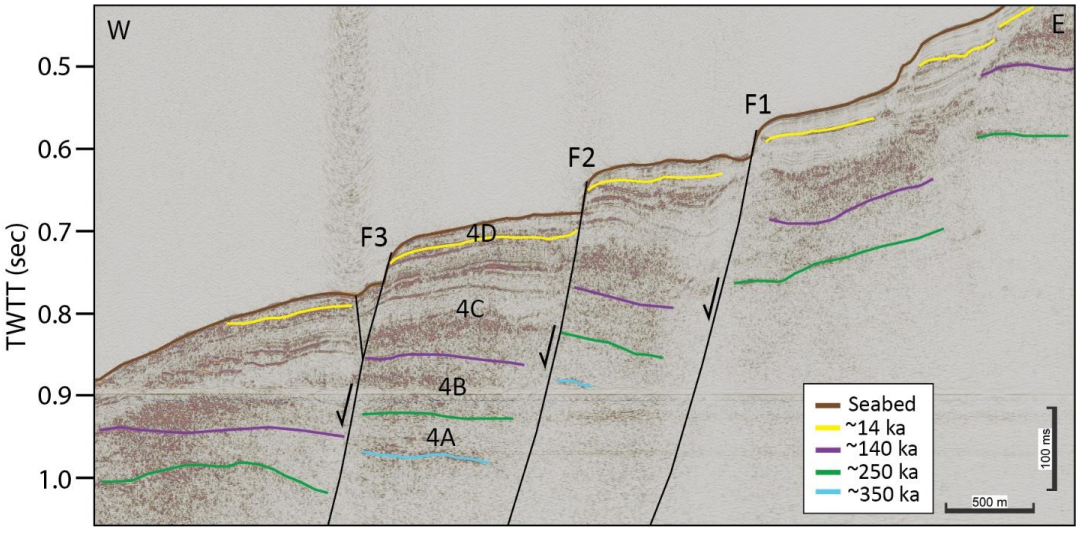

Figure 5: High-resolution seismic section conducted in this study. Faults analyzed in this study are marked as black lines (same faults presented in Fig. 3). Subdivision of Unit 4 into four sub-units (4a-4d). Base unit 4A (light blue horizon) is dated to 350 ka; Base unit 4B (green horizon) is dated to 250 ka; Base unit 4C (purple horizon) is dated to 140 ka; Base unit 4D (yellow horizon) is dated to 14 ka. For the location of the line, see Figure 1.

4.2 Displacement rates

First, we performed backward restoration of fault movement since 1.8 Ma on four faults identified in the industrial, relatively low-resolution seismic survey (e.g., Fig. 3); results of the displacement history and displacement rates are shown in Fig. 6a-b. Then, we performed the same analysis on the same faults (Fig. 5) utilizing the new stratigraphic subdivision of Unit 4 to 4a, 4b, 4c, and 4d (Fig. 6c-d). These results demonstrate that when slip rates are averaged over 350 ky, the obtained values are 0.1-0.25 m/ky, whereas higher-resolution analysis reveals that these average values can

https://doi.org/10.5194/egusphere-2025-6041
Preprint. Discussion started: 30 January 2026

be separated into much lower values for Units 4b-c and much higher values for Unit 4d. For practical purposes, considering the most recent displacements, slip rates have increased 10-fold.

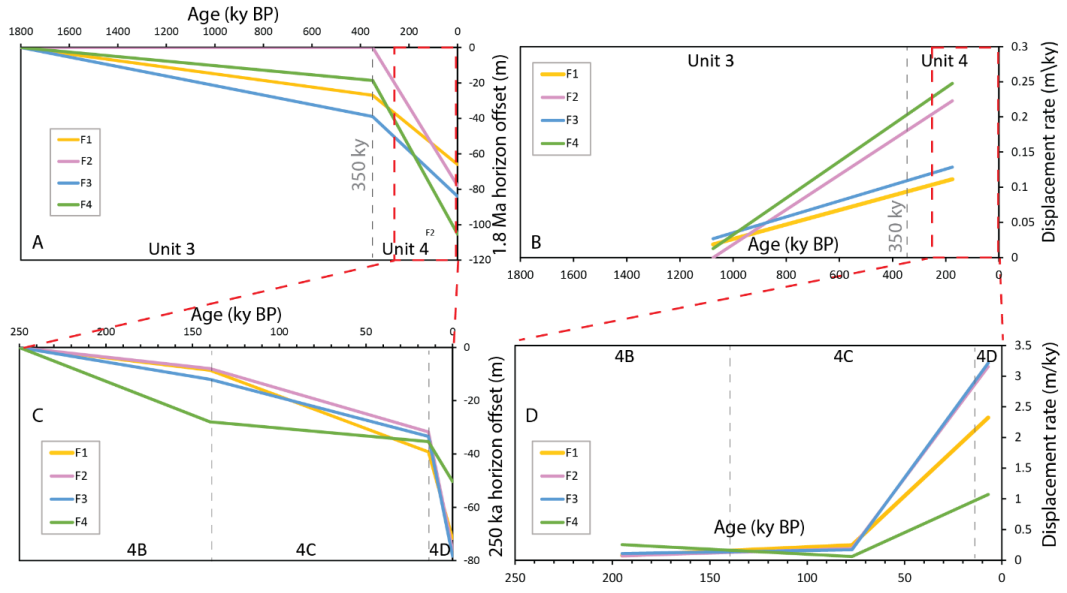

Figure 6: (A) Displacement history of the 1.8 Ma horizon identified in the industrial, relatively low-resolution seismic survey. (B) Displacement rates based on A. (C) Detailed presentation of Unit 4 subdivided into four subunits (4B-4D), based on high-resolution data collected in this study. (D) Detailed displacement rates of the subdivided Unit 4. Note the relatively high rates averaged over the last 14 ky (Unit 4D).

In a wider view (Fig. 7), downslope faults located above the salt wedge (Group 1 in Laor and Gvirtzman, 2023), indicate the highest slip rates during deposition of Unit 2 (2.6-1.8 Ma) and a decrease ever since (Elfassi et al., 2019). However, upslope faults located landward of the salt wedge (Group 2 in Laor and Gvirtzman, 2023) illustrate increased activity in the last 350 ky and

https://doi.org/10.5194/egusphere-2025-6041
Preprint. Discussion started: 30 January 2026

292 especially in the last 14 ky. This result highlights the hazard posed by Group 2 even more than
293 estimated by Laor and Gvirtzman (2023).

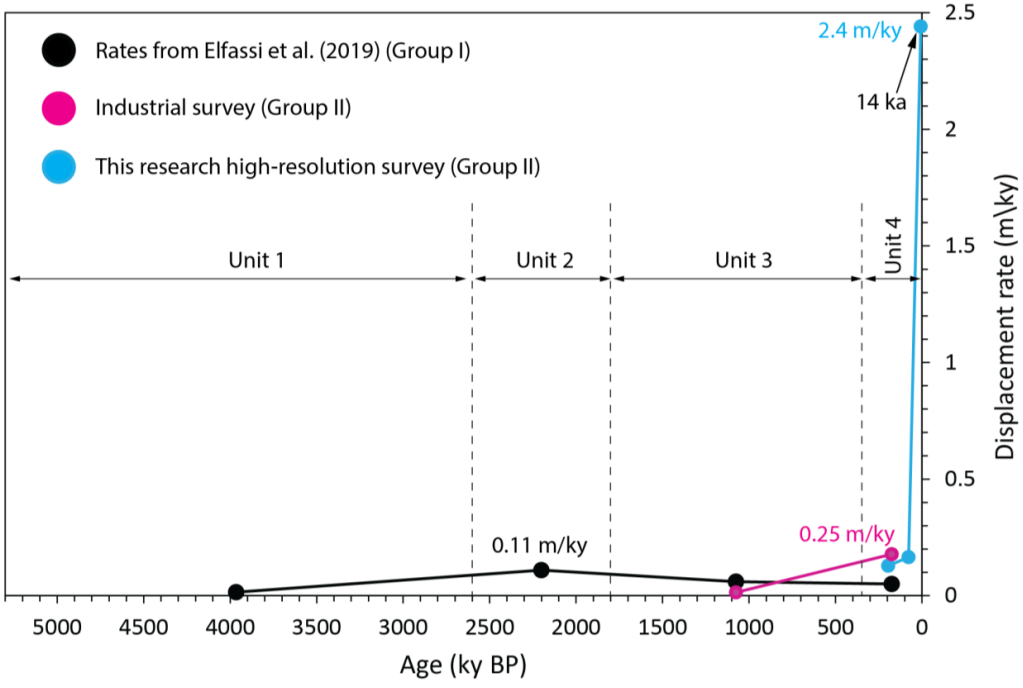

294

295 *Figure 7: Summary graph of displacement rates throughout the entire history of salt tectonics in*
296 *the Levant Basin. Classification of faults into two groups follows Laor and Gvirtzman (2023).*
297 *Displacement rates for Group I were calculated by Elfassi et al. (2019), reached 0.11 m/ky,*
298 *averaged over the Unit 2 period (2.6 Ma-1.8 Ma). Displacement rates for Group II were calculated*
299 *in this study based on industrial data, reaching 0.25 m/ky averaged over the Unit 4 period (350*
300 *ka-present). When recalculated using the new high-resolution data from this study, Group II*
301 *displacement rates average 2.4 m/ky over the last ~14 ky, a 10-fold increase compared to*
302 *calculations based on industrial data.*

https://doi.org/10.5194/egusphere-2025-6041
Preprint. Discussion started: 30 January 2026

5. Discussion

5.1 Sedimentation vs. displacement rates

Considering Unit 4 as a whole, its average sedimentation rate in the area of the analyzed faults is 2 m/ky (Laor and Gvirtzman, 2023), which is an order of magnitude faster than the average slip rates (0.25 m/ky). This means that on a 350 ky scale, fault scarps are expected to be completely buried. Therefore, the observed noticeable fault scarps (tens of meters high; Fig 8a) must indicate that displacement rates are non-linear and that a very recent rapid slip has created a fault step that has not yet been buried (Fig. 8a). However, a simple calculation shows that even the high slip rates inferred for the last 14 ky are insufficient to explain the observed fault scarps unless the fault scarps formed much after 14 ky. If faults move in a constant velocity (creep motion) of 2.5 m/ky, with a burial rate of 2 m/ky (Laor and Gvirtzman, 2023), the expected height of the fault scarp after 14 ky should be ~7 m, whereas in reality the observed fault scarps are a few times larger. This means that fault scarps must have formed in very recent seismic slip events or during recent rapid creep (Fig. 8b). This conclusion is supported by the striking similarity between the displacement patterns observed for the 14 ky horizon and the present-day bathymetric offset, which is approximately 25 m (Figure 8a).

https://doi.org/10.5194/egusphere-2025-6041
Preprint. Discussion started: 30 January 2026

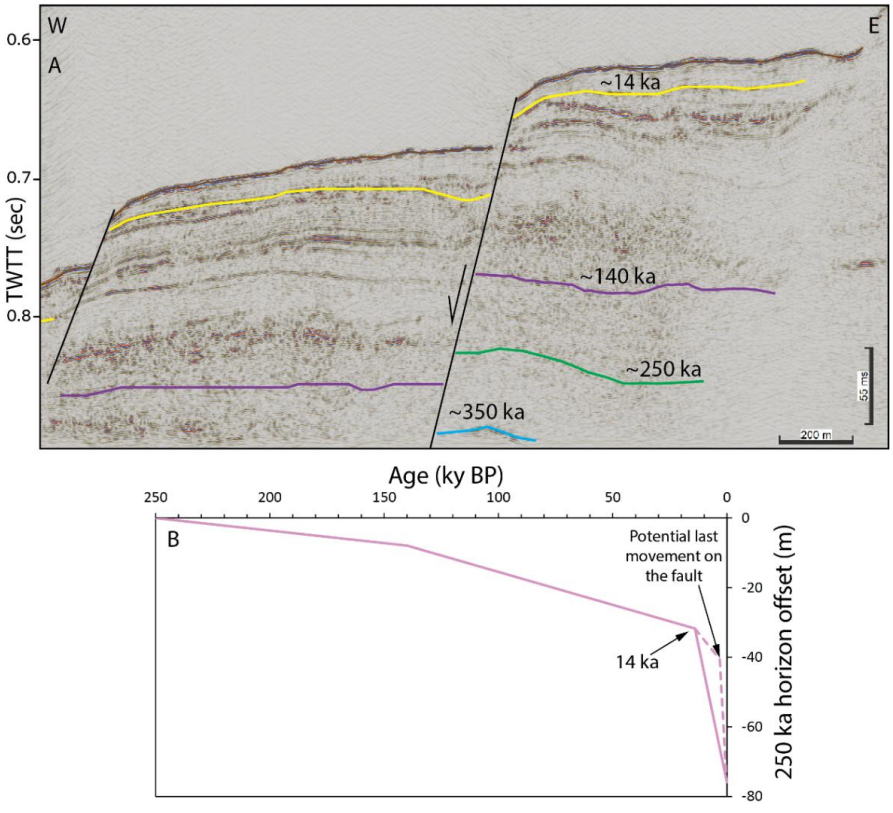

Figure 8: (A) Location of fault F2 (highlighted in black). (B) Displacement history of fault F2, showing significant displacement at 14 ka. Based on displacement-to-sedimentation rate ratios calculated for various scenarios described in the text, the most recent displacement on this fault likely occurred within the last 14 ky (indicated by dashed pink line).

Two additional factors complicate the simple comparison between sedimentation and displacement. First, several of the horizons used for offset measurements show truncation and may

https://doi.org/10.5194/egusphere-2025-6041
Preprint. Discussion started: 30 January 2026

represent erosional unconformities. Any removal of a section across these surfaces would alter the apparent offset and could either exaggerate or reduce the reconstructed slip. Second, the assumption of constant sedimentation rates within subunits is an approximation. Rates may have varied within Unit 4, and such variations would influence both burial and the interpreted timing of scarp formation.

The preservation of large fault scarps may also reflect episodes of erosion or non-deposition on the hanging wall or footwall. Submarine slides, which are common throughout the section, could reset or locally enhance topography without requiring sustained high slip rates. These processes offer alternative pathways to maintain relief even where average sedimentation is high.

The fault activity responsible for the current seafloor expression may have occurred much more recently than 14 ky - potentially even within historical times - or represents a combination of episodic slip events and varying sedimentation rates (Figure 8b). This temporal uncertainty has important implications for seismic hazard assessment, as the preservation of the prominent fault scarp indicates very recent fault activity that cannot be adequately constrained with our current chronological framework.

5.2 Correlation with sea level changes

The remarkable preservation of the 25 m fault scarp on the present-day seafloor, despite high sedimentation rates, raises a fundamental question: why did the activity of these faults rise so dramatically during the last 14 ky? Our hypothesis is that this acceleration is intrinsically linked to the steep post-glacial sea-level rise of 120 m. To further examine this hypothesis, we extended our analysis backward in time and illustrated a correlation between sea-level changes and fault

https://doi.org/10.5194/egusphere-2025-6041
Preprint. Discussion started: 30 January 2026

motion along three upslope faults (Fig. 9). The colored dashed lines in Figure 9b represent reconstructed motion across the faults, with age anchors at 250 ky, 140 ky, and 14 ky, corresponding to peak glacial periods, and linear age interpolation between these points based on relative unit thicknesses (Fig, 9a), assuming constant sedimentation rates within subunits. Comparison of the fault motions to the sea-level curve indicates a noticeable correlation between post-glacial sea-level rise and increased slip rates.

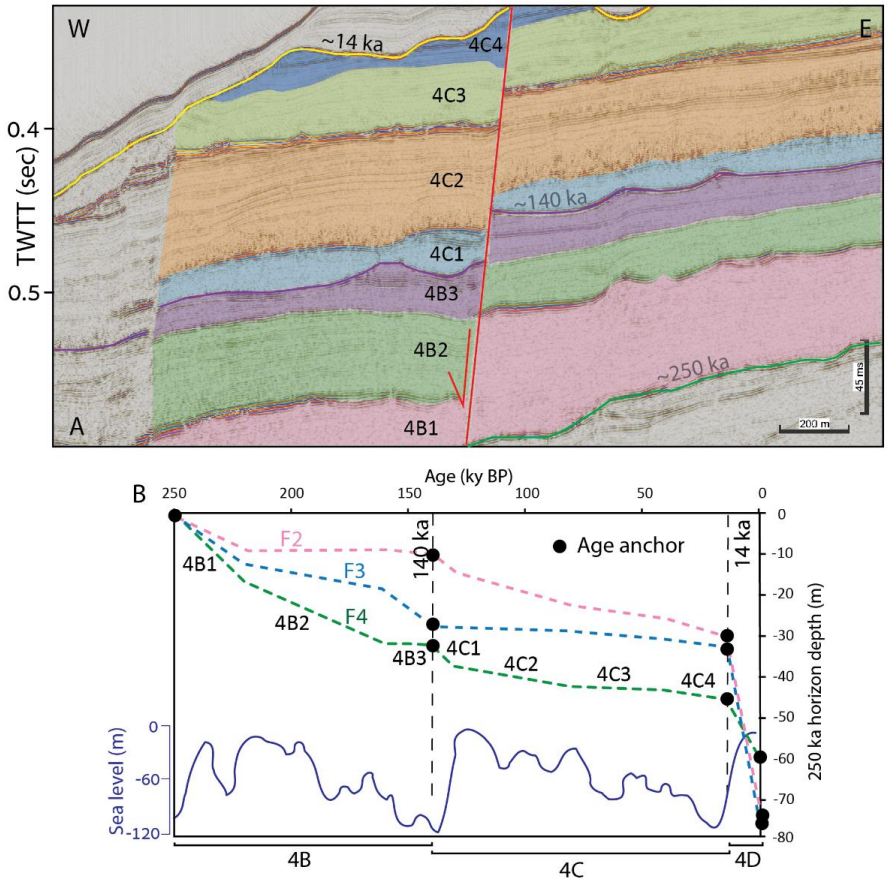

https://doi.org/10.5194/egusphere-2025-6041
Preprint. Discussion started: 30 January 2026

Figure 9: (A) Example of subdivision into undated sub-units for one of the faults (F4). (B) Correlation between displacement histories of F2, F3, and F4 faults and sea level change. Black dots indicate age anchor points. Between these points, the interpolated ages were calculated based on the ratio of unit thickness to time. Fault activity rates increase during periods of sea level change. Note that the displacements do not account for portions removed by erosion; therefore, original displacements may have been originally larger (for example, at 140 ka).

Nonetheless, it is still uncertain whether the observed fault acceleration responds to the onset of sea-level rise or legs sometime after the age of minimal sea level. This ambiguity stems from both the resolution limits of the data and the unknown lag time between environmental forcing and structural response. In any case, it seems clear that fault activity follows a cyclic pattern coinciding with glacial-interglacial transitions.

Because sea level has been relatively stable over the last ~7 ky, any very recent slip that contributes to the present-day scarp height may require an additional trigger unrelated to eustatic forcing, such as localized pore-pressure changes, internal salt-tectonic dynamics, or other short-term processes not resolved here. In light of our results, we propose that coupling between sea-level fluctuations and fault activity should be systematically tested along additional continental margins.

5.3 Implementation for hazard assessment

A fundamental challenge in offshore geohazard assessment arises when planned infrastructure must cross fault zones. One approach is to apply probabilistic fault displacement hazard analysis (PFDHA, Youngs et al., 2003), but this requires knowledge about magnitude-frequency

https://doi.org/10.5194/egusphere-2025-6041
Preprint. Discussion started: 30 January 2026

relationships, which is frequently unavailable. A more common alternative is to base hazard estimates on slip rates measured from displacements across the youngest possible stratigraphic horizon; however, this is resolution-dependent, as illustrated here. While measurements of the 350 ky horizon yield average values of 0.25 m/ky, the post-glacial stratigraphy indicates 10-fold higher values. In addition, the observed correlation between sea-level rise and increased fault activity during the late Pleistocene suggests that site-specific surveys must consider post-glacial slip rates, at least in thin-skinned faults, and possibly in other cases as well.

Continuing this line of thinking, we further raise the possibility that an additional increase in stratigraphic resolution is needed to separate the rapid sea-level rise at 18-8 ka from the relatively stable sea-level in the last 7 ky. Figure 10 illustrates that such a distinction between early and late Holocene could further change the calculated slip rates, with higher values in the early interval (sea-level rises) and lower values recently (stable sea-level). In other words, an additional increase in resolution may ease planning by allowing the use of less strict values, calling for the integration of ultra-high-resolution sub-seabed seismic with core dating. Conversely, despite our hypothesis about increased faulting during sea level rise, increasing resolution may also work the other way around and show that slip rates may have increased in the late Holocene; we will not know until we measure.

https://doi.org/10.5194/egusphere-2025-6041
Preprint. Discussion started: 30 January 2026

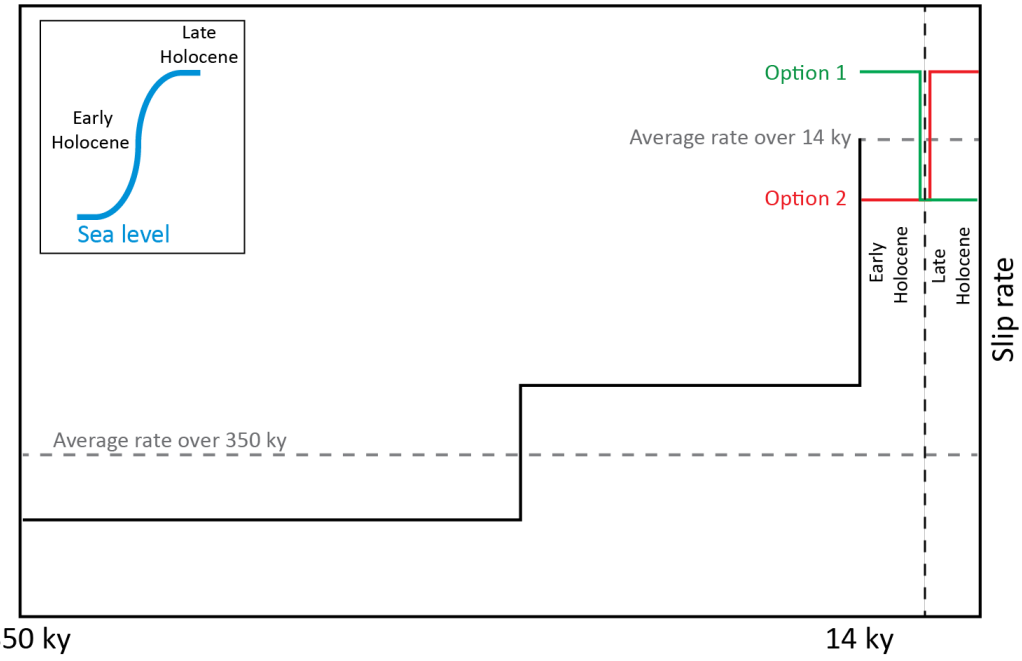

Figure 10: Illustrated plot showing increased displacement rates for each time interval based on average displacement rates. The green and red curves show two alternative scenarios for variations in displacement rate over the last 14 ky, both yielding the same average rate. Note that Option 1 (green) would provide relief in geohazard planning due to sea level stability in the late Holocene, while Option 2 (red) would worsen it. This graph highlights the importance of enhanced temporal resolution for geohazard assessment.

6. Conclusions

This study demonstrates that stratigraphic resolution has a fundamental impact on hazard assessment for marine infrastructure crossing active fault zones. By increasing temporal resolution

https://doi.org/10.5194/egusphere-2025-6041
Preprint. Discussion started: 30 January 2026

from 350 ky to 14 ky using high-resolution seismic reflection data, we obtained fault slip rates more than 10 times higher than previously reported long-term averages. This finding reveals that conventional hazard surveys, which rely on older stratigraphic horizons, may significantly underestimate current fault activity and associated infrastructure risks.

The preservation of 25-meter fault scarps despite high sedimentation rates indicates very recent fault activity, potentially within historical times. Our analysis shows a strong correlation between glacial-interglacial sea-level cycles and fault displacement rates. We propose that pore pressure changes during rapid sea-level rise destabilize fault zones, with broad implications for Mediterranean continental margins underlain by Messinian salt deposits.

For infrastructure design, long-term averaged slip rates of 0.25 mm/yr may be inadequate compared to recent rates exceeding 2.4 mm/yr. However, if sea-level forcing drives this acceleration, current high rates may represent a transient peak, suggesting higher temporal resolution could refine hazard estimates.

The coupling between climatic forcing and thin-skinned fault activity introduces new considerations for geohazard forecasting. Our findings suggest fault activity may respond predictably to environmental forcing, with direct implications for infrastructure planning during continued anthropogenic sea-level rise.

Future research should extend this approach to additional Mediterranean sites and subdivide Holocene sediments to quantify environmental-tectonic relationships, ultimately improving predictive models for marine geohazard assessment.

https://doi.org/10.5194/egusphere-2025-6041
Preprint. Discussion started: 30 January 2026

7. Data availability

The seismic datasets used in this article comprise industrial data and high-resolution multi-channel reflection data collected specifically for this study. Additional details can be obtained from the Israel Ministry of Energy (https://prime.energy.gov.il/).

8. Author contribution

ML collected and processed the reflection data, formal analysis, visualization of results, wrote the original draft, and conceptualization. **ZG** supervised, formal analysis, visualization of results, wrote the original draft, and conceptualization. **OG** collected and processed the reflection data, reviewed and edited the draft. **YM** collected the reflection data, reviewed and edited the draft. **OK** collected the reflection data, reviewed and edited the draft.

9. Competing interests

At least one of the co-authors is a member of the editorial board of NHESS

10. Acknowledgments

We thank HIS Markit (London, UK) for providing the Kingdom academic licenses for seismic interpretation. We thank Emerson-Paradigm (now Aspentech SSE) for sponsoring their software. We thank the crew of R/V Bat-Galim (IOLR) for their help with the marine survey. This research was funded by the Israeli Ministry of Energy.

11. References

Almagor, G., Gill, D. and Perath, I., 2000. Marine sand resources offshore Israel. Marine georesources & geotechnology, 18(1), pp.1-42.

https://doi.org/10.5194/egusphere-2025-6041
Preprint. Discussion started: 30 January 2026

Angell, M.M., Hanson, K., Swan, F.H., Youngs, R. and Abramson, H., 2003, May. Probabilistic fault displacement hazard assessment for flowlines and export pipelines, Mad Dog and Atlantis field developments, deepwater Gulf of Mexico. In Offshore technology conference (pp. OTC-15402). OTC.

Ben-Avraham, Z., 1978, The structure and tectonic setting of the Levant continental margin, Eastern Mediterranean, Tectonophysics, 46(3-4), 313-331.

Ben-Gai, Y., Ben-Avraham, Z., Buchbinder, B. and Kendall, C.G.S.C., 2005. Post-Messinian evolution of the Southeastern Levant Basin based on two-dimensional stratigraphic simulation. Marine Geology, 221(1-4), pp.359-379.

Ben Zeev, Y., and Gvirtzman, Z., 2020, When two salt tectonics systems meet: Gliding downslope the Levant margin and salt out-squeezing from under the Nile delta, Tectonics, 39(12), e2019TC005715.

Bender, B. and Perkins, D.M., 1987. SEISRISK III: a computer program for seismic hazard estimation (No. 1772). US Government Printing Office.

Bertoni, C., and Cartwright, J. A., 2006, Controls on the basinwide architecture of late Miocene (Messinian) evaporites on the Levant margin (Eastern Mediterranean), Sedimentary Geology, 188, 93-114.

Bondevik, S., Stormo, S.K. and Skjerdal, G., 2012. Green mosses date the Storegga tsunami to the chilliest decades of the 8.2 ka cold event. Quaternary science reviews, 45, pp.1-6.

Brothers, D.S., Luttrell, K.M. and Chaytor, J.D., 2013. Sea-level–induced seismicity and submarine landslide occurrence. Geology, 41(9), pp.979-982.

https://doi.org/10.5194/egusphere-2025-6041
Preprint. Discussion started: 30 January 2026

Buchbinder, B., Martinotti, G. M., Siman-Tov, R., and Zilberman, E., 1993, Temporal and spatial relationships in Miocene reef carbonates in Israel, Palaeogeography, Palaeoclimatology, Palaeoecology, 101(1-2), 97-116.

Buchbinder, B., and Zilberman, E., 1997, Sequence stratigraphy of Miocene-Pliocene carbonate-siliciclastic shelf deposits in the eastern Mediterranean margin (Israel): effects of eustasy and tectonics, Sedimentary Geology, 112(1-2), 7-32.

Bryn, P., Berg, K., Forsberg, C.F., Solheim, A. and Kvalstad, T.J., 2005. Explaining the Storegga slide. Marine and Petroleum Geology, 22(1-2), pp.11-19.

Carmel, Z., Inman, D. L., and Golik, A., 1985, Characteristics of storm waves off the Mediterranean coast of Israel, Coastal Engineering, 9(1), 1-19.

Cartwright, J. A., and Jackson, M. P. A., 2008, Initiation of gravitational collapse of an evaporite basin margin: The Messinian saline giant, Levant Basin, eastern Mediterranean, Geological Society of America Bulletin, 120(3-4), 399-413.

Cartwright, J., Jackson, M., Dooley, T., and Higgins, S., 2012, Strain partitioning in gravity-driven shortening of a thick, multilayered evaporite sequence.

Cornell, C.A., 1968. Engineering seismic risk analysis. Bulletin of the seismological society of America, 58(5), pp.1583-1606.

Clark, I. R., and Cartwright, J. A., 2009, Interactions between submarine channel systems and deformation in deepwater fold belts: Examples from the Levant Basin, Eastern Mediterranean sea, Marine and Petroleum Geology, 26(8), 1465-1482.

https://doi.org/10.5194/egusphere-2025-6041
Preprint. Discussion started: 30 January 2026

Elfassi, Y., Gvirtzman, Z., Katz, O., and Aharonov, E., 2019, Chronology of post-Messinian faulting along the Levant continental margin and its implications for salt tectonics, Marine and Petroleum Geology, 109, 574-588.

Emery, K. O., Neev, D., and Bentor, Y. K., 1960, Mediterranean beaches of Israel, Jerusalem: Geological Survey of Israel.

Frey-Martínez, J., Cartwright, J. and James, D., 2006. Frontally confined versus frontally emergent submarine landslides: A 3D seismic characterisation. Marine and Petroleum Geology, 23(5), pp.585-604.

Gadol, O., Tibor, G., ten Brink, U., Hall, J. K., Groves-Gidney, G., Bar-Am, G., ... and Makovsky, Y., 2020, Semi-automated bathymetric spectral decomposition delineates the impact of mass wasting on the morphological evolution of the continental slope, offshore Israel, Basin Research, 32(5), 1156-1183.

Gadol, O., Katz, O., Kanari, M. and Makovsky, Y., 2025. Millennial-scale phased submarine retrogressive collapse of the owl slide complex. Geomorphology, p.109973.

Galloway, W.E., 1989. Genetic stratigraphic sequences in basin analysis II: application to northwest Gulf of Mexico Cenozoic basin. AAPG bulletin, 73(2), pp.143-154.

Garfunkel, Z., Almagor, G., and Arad, A., 1979, The Palmahim disturbance and its regional setting, Geol. Surv. Israel Bull., v. 72, p. 1–58.

Garfunkel, Z., 1984, Large-scale submarine rotational slumps and growth faults in the eastern Mediterranean, Marine Geology, 55(3-4), 305-324.

https://doi.org/10.5194/egusphere-2025-6041
Preprint. Discussion started: 30 January 2026

507 Garfunkel, Z., and Almagor, G., 1984, Geology and structure of the continental margin off
508 northern Israel and the adjacent part of the Levantine Basin, Marine Geology, 62(1-2), 105-131.

509 Goldsmith, V., and Golik, A., 1980, Sediment transport model of the southeastern Mediterranean
510 coast, Marine Geology, 37(1-2), 147-175.

511 Gradmann, S., Hübscher, C., Ben-Avraham, Z., Gajewski, D., and Netzeband, G., 2005, Salt
512 tectonics off northern Israel, Marine and Petroleum Geology, 22(5), 597-611.

513 Gvirtzman, G. and Buchbinder, B., 1978. The Late Miocene Marine Transgression in the Be'er
514 Sheva Area. ISRAEL JOURNAL OF EARTH-SCIENCES, 27, pp.72-82.

515 Gvirtzman, Z., Reshef, M., Buch-Leviatan, O., and Ben-Avraham, Z., 2013, Intense salt
516 deformation in the Levant Basin in the middle of the Messinian Salinity Crisis, Earth and Planetary
517 Science Letters, 379, 108-119.

518 Gvirtzman, Z., Reshef, M., Buch-Leviatan, O., Groves-Gidney, G., Karcz, Z., Makovsky, Y., and
519 Ben-Avraham, Z., 2015 Bathymetry of the Levant basin: interaction of salt-tectonics and surficial
520 mass movements, Marine Geology, 360, 25-39.

521 Gvirtzman, Z., Heida, H., Garcia-Castellanos, D., Bar, O., Zucker, E., and Enzel, Y., 2022, Limited
522 Mediterranean sea-level drop during the Messinian salinity crisis inferred from the buried Nile
523 canyon, Communications Earth & Environment, 3(1), 216.

524 Haflidason, H., Lien, R., Sejrup, H.P., Forsberg, C.F. and Bryn, P., 2005. The dating and
525 morphometry of the Storegga Slide. Marine and Petroleum Geology, 22(1-2), pp.123-136.

526 Hall, J. K., 1994. Digital shaded-relief map of Israel and environs, Agaf ha-medidot.

https://doi.org/10.5194/egusphere-2025-6041
Preprint. Discussion started: 30 January 2026

Hamdani, I., Aharonov, E., Olive, J. A., Parez, S., and Gvirtzman, Z., 2021 Initiating salt tectonics by tilting: Viscous coupling between a tilted salt layer and overlying brittle sediment, Journal of Geophysical Research: Solid Earth, 126(7), e2020JB021503.

Hamann, Y., Ehrmann, W., Schmiedl, G., Krüger, S., Stuut, J.B. and Kuhnt, T., 2008. Sedimentation processes in the Eastern Mediterranean Sea during the Late Glacial and Holocene revealed by end-member modelling of the terrigenous fraction in marine sediments. Marine Geology, 248(1-2), pp.97-114.

Hough, G., Green, J., Fish, P., Mills, A. and Moore, R., 2011. A geomorphological mapping approach for the assessment of seabed geohazards and risk. Marine Geophysical Research, 32(1), pp.151-162.

Hsü, K.J., 1977. Tectonic evolution of the Mediterranean basins. In The Ocean Basins and Margins: Volume 4A The Eastern Mediterranean (pp. 29-75). Boston, MA: Springer US.

Hübscher, C., and Netzeband, G. L., 2017, Evolution of a young salt giant: the example of the Messinian evaporites in the Levantine Basin, In The Mechanical Behavior of Salt–Understanding of THMC Processes in Salt (pp. 175-182). CRC Press.

Hunt, D. and Tucker, M.E., 1992. Stranded parasequences and the forced regressive wedge systems tract: deposition during base-level'fall. Sedimentary Geology, 81(1-2), pp.1-9.

Katz, O., Reuven, E. and Aharonov, E., 2015. Submarine landslides and fault scarps along the eastern Mediterranean Israeli continental-slope. Marine Geology, 369, pp.100-115.

Klein, M., Zviely, D., Kit, E., and Shteinman, B., 2007, Sediment transport along the coast of Israel: examination of fluorescent sand tracers, Journal of Coastal Research, 23(6), 1462-1470.

https://doi.org/10.5194/egusphere-2025-6041
Preprint. Discussion started: 30 January 2026

548 Kvalstad, T.J., 2007, April. What is the current" best practice" in offshore geohazard
549 investigations? A State-of-the-art review. In Offshore technology conference (pp. OTC-18545).
550 OTC.

551 Laor, M., and Gvirtzman, Z., 2023, Classifying marine faults for hazard assessment offshore Israel:
552 a new approach based on fault size and vertical displacement, Natural Hazards and Earth System
553 Sciences, 23(1), 139-158.

554 Laor, M. and Gvirtzman, Z., 2025. The role of pre-salt relief and detachment surfaces in thin-
555 skinned tectonics: The Palmahim rapidly gliding corridor and the Dor rollover anticline, offshore
556 Israel. Geological Society of America Bulletin.

557 Lee, H.J., 2009. Timing of occurrence of large submarine landslides on the Atlantic Ocean margin.
558 Marine Geology, 264(1-2), pp.53-64.

559 Locat, J. and Lee, H.J., 2002. Submarine landslides: advances and challenges. Canadian
560 Geotechnical Journal, 39(1), pp.193-212.

561 Loncke, L., Gaullier, V., Mascle, J., Vendeville, B., and Camera, L., 2006, The Nile deep-sea fan:
562 an example of interacting sedimentation, salt tectonics, and inherited subsalt paleotopographic
563 features, Marine and Petroleum Geology, 23(3), 297-315.

564 Luttrell, K. and Sandwell, D., 2010. Ocean loading effects on stress at near shore plate boundary
565 fault systems. Journal of Geophysical Research: Solid Earth, 115(B8).

566 Manzi, V., Gennari, R., Lugli, S., Persico, D., Reghizzi, M., Roveri, M., Schreiber, B.C., Calvo,
567 R., Gavrieli, I. and Gvirtzman, Z., 2018. The onset of the Messinian salinity crisis in the deep
568 Eastern Mediterranean basin. Terra Nova, 30(3), pp.189-198.

https://doi.org/10.5194/egusphere-2025-6041
Preprint. Discussion started: 30 January 2026

Mart, Y., and Ben Gai, Y., 1982, Some depositional patterns at continental margin of southeastern Mediterranean Sea, AAPG Bulletin, 66(4), 460-470.

Mart, Y., and Ryan, W., 2007, The Levant slumps and the Phoenician structures: Collapse features along the continental margin of the southeastern Mediterranean Sea, Marine Geophysical Researches, 28, 297-307.

Martinez, J. F., Cartwright, J., and Hall, B., 2005, 3D seismic interpretation of slump complexes: examples from the continental margin of Israel, Basin Research, 17(1), 83-108.

Maslin, M., Owen, M., Day, S. and Long, D., 2004. Linking continental-slope failures and climate change: Testing the clathrate gun hypothesis. Geology, 32(1), pp.53-56.

Masson, D.G., Harbitz, C.B., Wynn, R.B., Pedersen, G. and Løvholt, F., 2006. Submarine landslides: processes, triggers and hazard prediction. Philosophical Transactions of the Royal Society A: Mathematical, Physical and Engineering Sciences, 364(1845), pp.2009-2039.

McGuire, R.K., 1976. FORTRAN computer program for seismic risk analysis (No. 76-67). US Geological Survey,.

Meilijson, A., Steinberg, J., Hilgen, F., Bialik, O.M., Waldmann, N.D. and Makovsky, Y., 2018. Deep-basin evidence resolves a 50-year-old debate and demonstrates synchronous onset of Messinian evaporite deposition in a non-desiccated Mediterranean. Geology, 46(3), pp.243-246.

Mitrovica, J.X. and Peltier, W.R., 1991. On postglacial geoid subsidence over the equatorial oceans. Journal of Geophysical Research: Solid Earth, 96(B12), pp.20053-20071.

Neev, D., Almagor, G., Arad, A., Ginzburg, A., and Hall, J. K., 1976, The geology of the southeastern Mediterranean Sea (No. 68), Geological Survey of Israel.

https://doi.org/10.5194/egusphere-2025-6041
Preprint. Discussion started: 30 January 2026

Netzeband, G. L., Hübscher, C. P., and Gajewski, D., 2006, The structural evolution of the Messinian evaporites in the Levantine Basin, Marine Geology, 230(3-4), 249-273.

On, G.N., 2016. Guidance Notes on Subsea Pipeline Route Determination. ABS (American Bureau of Shipping).

Owen, M., Day, S. and Maslin, M., 2007. Late Pleistocene submarine mass movements: occurrence and causes. Quaternary Science Reviews, 26(7-8), pp.958-978.

Paull, C.K., Buelow, W.J., Ussler III, W. and Borowski, W.S., 1996. Increased continental-margin slumping frequency during sea-level lowstands above gas hydrate–bearing sediments. Geology, 24(2), pp.143-146.

Prior, D.B. and Hooper, J.R., 1999. Sea floor engineering geomorphology: recent achievements and future directions. Geomorphology, 31(1-4), pp.411-439.

Rowan, M.G., Jackson, M.P. and Trudgill, B.D., 1999. Salt-related fault families and fault welds in the northern Gulf of Mexico. AAPG bulletin, 83(9), pp.1454-1484.

Ryan, W.B., 2009. Decoding the Mediterranean salinity crisis. Sedimentology, 56(1), pp.95-136.

Schattner, U., Lazar, M., Tibor, G., Ben-Avraham, Z. and Makovsky, Y., 2010. Filling up the shelf—A sedimentary response to the last post-glacial sea rise. Marine Geology, 278(1-4), pp.165-176.

Schattner, U., Gurevich, M., Kanari, M., and Lazar, M., 2015, Levant jet system—effect of post LGM seafloor currents on Nile sediment transport in the eastern Mediterranean, Sedimentary Geology, 329, 28-39.

https://doi.org/10.5194/egusphere-2025-6041
Preprint. Discussion started: 30 January 2026

Schattner, U., and Lazar, M., 2016, Hierarchy of source-to-sink systems—Example from the Nile distribution across the eastern Mediterranean, Sedimentary geology, 343, 119-131.

Segev, A., Rybakov, M., Lyakhovsky, V., Hofstetter, A., Tibor, G., Goldshmidt, V. and Avraham, Z.B., 2006. The structure, isostasy and gravity field of the Levant continental margin and the southeast Mediterranean area. Tectonophysics, 425(1-4), pp.137-157.

Simpson, D.W., 1976. Seismicity changes associated with reservoir loading. Engineering Geology, 10(2-4), pp.123-150.

Smith, D.E., Harrison, S. and Jordan, J.T., 2013. Sea level rise and submarine mass failures on open continental margins. Quaternary Science Reviews, 82, pp.93-103.

Steinberg, J., Gvirtzman, Z., Folkman, Y., and Garfunkel, Z., 2011, Origin and nature of the rapid late Tertiary filling of the Levant Basin, Geology, 39(4), 355-358.

Talwani, P., 1997. On the nature of reservoir-induced seismicity. Pure and applied Geophysics, 150(3), pp.473-492.

Tappin, D.R., 2010. Digital elevation models in the marine domain: investigating the offshore tsunami hazard from submarine landslides.

Tibor, G., Ben-Avraham, Z., Steckler, M., and Fligelman, H., 1992, Late Tertiary subsidence history of the Southern Levant Margin, Eastern Mediterranean Sea, and its implications to the understanding of the Messinian event, Journal of Geophysical Research: Solid Earth, 97(B12), 17593-17614.

Trincardi, F., Cattaneo, A., Correggiari, A., Mongardi, S., Breda, A. and Asioli, A., 2003. Submarine slides during relative sea level rise: two examples from the eastern Tyrrhenian margin.

https://doi.org/10.5194/egusphere-2025-6041
Preprint. Discussion started: 30 January 2026

In Submarine Mass Movements and Their Consequences: 1st International Symposium (pp. 469-478). Dordrecht: Springer Netherlands.

Urlaub, M., Talling, P.J. and Masson, D.G., 2013. Timing and frequency of large submarine landslides: implications for understanding triggers and future geohazard. Quaternary Science Reviews, 72, pp.63-82.

Vail, P.R., Mitchum Jr., R.M., Todd, R.G., Widmier, J.M., Thompson III., S., Sangree, J.B., Bubb, J.N. and Hatlelid, W.G., 1977. Seismic Strati-Graphy and Global Changes of Sea Level. In: Payton, C.E., Ed., Seismic Stratigraphy—Applications to Hydrocarbon Exploration, Vol. 26, American Association of Petroleum Geology Memoir, Tulsa, 49-212.

Wien, K., Holz, C., Kölling, M. and Schulz, H.D., 2006. Age models for pelagites and turbidites from the Cap Timiris Canyon off Mauritania. Marine and Petroleum Geology, 23(3), pp.337-352.

Wong, I.G. and Stepp, C., 1998. Probabilistic seismic hazard analyses for fault displacement and vibratory ground motion at Yucca Mountain, Nevada. Milestone SP32IM3, September, 23, p.1998.

Youngs, R.R., Arabasz, W.J., Anderson, R.E., Ramelli, A.R., Ake, J.P., Slemmons, D.B., McCalpin, J.P., Doser, D.I., Fridrich, C.J., Swan III, F.H. and Rogers, A.M., 2003. A methodology for probabilistic fault displacement hazard analysis (PFDHA). Earthquake spectra, 19(1), pp.191-219.

Zucker, E., Gvirtzman, Z., Granjeon, D., Garcia-Castellanos, D., and Enzel, Y., 2021, The accretion of the Levant continental shelf alongside the Nile Delta by immense margin-parallel sediment transport, Marine and Petroleum Geology, 126, 104876.

https://doi.org/10.5194/egusphere-2025-6041
Preprint. Discussion started: 30 January 2026

651 Zviely, D., Sivan, D., Ecker, A., Bakler, N., Rohrlich, V., Galili, E., ... and Kit, E., 2006, Holocene
652 evolution of the Haifa Bay area, Israel, and its influence on ancient tell settlements, The Holocene,
653 16(6), 849-861.

654 Zviely, D., Kit, E., and Klein, M., 2007, Longshore sand transport estimates along the
655 Mediterranean coast of Israel in the Holocene, Marine geology, 238(1-4), 61-73.

656

657

658

659

660

661

662